**K. S. Zabolotnyi, Dr. Sc. (Tech.), Prof.,**
orcid.org/0000-0001-8431-0169,
**O. V. Panchenko, Cand. Sc. (Tech.), Assoc. Prof.,**
orcid.org/0000-0002-1664-2871,
**O. L. Zhupiiev,**
orcid.org/0000-0003-0531-2217,
**M. V. Polushyna, Cand. Sc. (Tech.), Assoc. Prof.,**
orcid.org/0000-0003-2853-0671

National Mining University, Dnipro, Ukraine, e-mail: mmf@ua.fm

## INFLUENCE OF PARAMETERS OF A RUBBER-ROPE CABLE ON THE TORSIONAL STIFFNESS OF THE BODY OF THE WINDING

**Purpose.** Development of a mathematical model of the stress-strain state of the body of the winding of the bobbin hoisting machine with rubber-rope cable.

**Methodology.** Methods of mathematical and computational experiment based on the finite element analysis are used.

**Findings.** To solve the problem of defining the torsional stiffness of the body of the winding of the rubber-rope cable (RRC), the physical model of the body of the winding was represented in the form of a composite in which the reinforcement is an infinitely thin spiral having stiffness characteristics of a metal rope and the matrix is a rubber sheath. After processing the results of the computational experiment using the computer finite element modeling method, an analytical expression for determining the torsional stiffness coefficient of the body of the winding of the RRC was obtained, the analysis of which shows that the stiffness of the body of the winding depends quadratically on its outer diameter, and the local stiffness depends little on the diameter. The danger of dynamic effects occurring in the bobbin hoist can take place at a large number of turns in the winding.

**Originality.** The regularities of the influence of the rubber-rope cable parameters on the torsional stiffness of the body of the winding have been established. The nonlinear character of changing the given stiffness characteristics of the RRC packet layers is caused by the peculiarity of interaction of the first packet layer with the bobbin surface. This interaction can be taken into account by applying the coefficient of a torsional stiffness hardening, for which an analytical expression was obtained by processing the results of the computational experiment.

**Practical value.** The developed mathematical model of determining the stiffness of the rubber-rope cable winding allows finding the parameters of the bobbin hoist, at which the danger of dynamic effects during the emergency and service braking caused by the torsional stiffness of the body of the winding is excepted.

**Keywords:** *bobbin hoisting machine, rubber-rope cable, multilayer winding, the body of the winding, torsional stiffness of the winding*

**Introduction.** The multilayer winding of the rubber-rope cable is one of the insufficiently explored elements of the bobbin hoisting machines, which has a high compliance and influences the dynamic processes in the hoisting installation. Because of the high compliance of the cable wound on the bobbin in a short branch, considerable oscillations of the lifting vessel can arise, which are dangerous for the possibility of its offset from the discharge curves. It follows from the foregoing that the evaluation of stiffness is an important problem, the solution of which is necessary for the research on dynamics of the hoisting installation.

**Analysis of the recent research and publications.** The works of V. P. Franchuk and K. A. Ziborov [1] are devoted to the elaboration of mathematical models of the mechanical systems with distributed and lumped parameters during stationary and non-stationary rectilinear motion. In the works of S. R. Ilin and V. I. Samusya [2, 3], I. O. Taran and I. Yu. Klymenko [4] the dependences of dynamic parameters on the parameters of the technical state of the individual links of the installation have been established on the basis of complex research studies. Carrying out the research of the mine hoists D. L. Kolosov [5] elaborated the methodical recommendations on the choice of rational parameters of the lift hoists with RRC.

In the works of K. S. Zabolotnyi [6] the problem of deformation of the bobbin winding under the action of a concentrated tangential force applied to the outer free end of a wound cable was solved. For this purpose, the finite element method was used, which took into account the spirality of the winding and the following assumptions: 1) the cable layers work together without slipping; 2) the real construction of the body of the winding has the form of a sequence of spiral layers of constant thickness corresponding in the stiffness characteristics to the ropes and the rubber matrix; 3) the rubber matrix operates in the linear deformation region; 4) the phenomena that occur with the rubber matrix, are similar to the properties of rubber in the abutment joints of the RRC.

As a result of computational experiments with a limited number of layers of the body of the winding (up to 20) two types of reaction were discovered. In case the stiffness of the rope was comparable to the stiffness of the rubber matrix, the deformations concentrated at the point where the cable descends from the bobbin, while the circumferential and radial displacements correspond to values of the same order. In conditions where the rope stiffness values were real, the body of the winding worked as a solid elastic body, which differs by an increased shear modulus in comparison to the same index of rubber. The magnitude of the shear is equal to the coefficient, which depends on the ratios $t/d$ and $h/d$ (here $d$ is the diameter of the rope, $t$ is the pitch of the rope, $h$ is the thickness of the cable), under conditions of loading the body with a twisting moment.

Based on the analysis of these experiments, an analytical shear model of the body of the winding was proposed, based on the following assumptions:

- its stiff layers are infinitely thin, they work only on extension-compression and do not have bending stiffness;

- of all the components of the displacement of points in the soft layers of winding, only angular displacement is taken into account;

- for a soft layer the linear law of the angle change in rigid layers is applied.

In order to characterize the changeability of the stress-strain state of the body of the winding in the circumferential coordinate, the following parameter is introduced

$$Z = \sqrt{E \cdot F_r \cdot j / (G_{sd} \cdot t \cdot R_0 \cdot \pi)}, \qquad (1)$$

where $E$ is the modulus of rope elasticity of elongation; $F_r$ is the cross-sectional area of the rope; $j$ is the number of turns; $Gsd$ is the reduced shear modulus of the body of the winding; $R_0$ is the radius of the shell.

Based on the computational study of the model, it was concluded that taking into account the real parameters of the RRC and the initial radius of the bobbin, if the criterion is $Z \geq 20$, the body of the winding shows itself as a homogeneous cylindrical body in torsion, and its rigidity is

$$C_{hcb} = 4\pi \cdot G_{sd} \cdot b / (\rho_j^2 - 1), \qquad (2)$$

where $\rho_j = r_j(2\pi)/R_0$; $b$ is the width of the body of the winding.

**Unresolved aspects of the problem.** Design parameters of bobbin hoisting installations with the RRC, intended for a depth of more than 2000 m, and with a load-carrying capacity of up to 400 tons, essentially differ from the parameters of bobbin hoists, which have been studied in the works mentioned above. This circumstance necessitates a deeper analysis of the stressed-strain state of the body of the winding when the tension of the hoisting cable is changed.

**The objective of the article** is to develop a mathematical model of the stress-strain state of the body of the winding of bobbin hoisting machines with a rubber-rope cable.

**Presentation of the main research.** When creating a finite-element model of the body of the winding, the following assumptions were made: 1) the rubber-rope cable is modeled as a sequence of non-interacting rubber-coated ropes; 2) the rope is modeled as a flat spiral-shaped body with a circular cross-section equal to the diameter of the cable; 3) the model of the rubber matrix is a hollow cylinder, and its diameter corresponds to the diameter of the shell and the outer diameter of the body of the winding, in which a spiral-shaped hole is cut, suitable for the model of the rope; 4) the rope and the rubber matrix interact without slipping; 5) the rubber matrix is rigidly connected to the shell; 6) in view of symmetry, half the body of the winding is considered; 7) because of the smallness of the ratio $h/R_0$, a linear tetrahedral finite element is used; 8) the load is applied to the linear section of the rope, which is smoothly connected to the spiral-shaped rope.

From the analysis of the works of predecessors it follows that in general case the torsional stiffness of the body of the winding can be represented as the stiffness of two series-connected springs. One of them corresponds to the torsional stiffness of a homogeneous body, and the other corresponds to a local deformation concentrated in the vicinity of the point of the rope descend. As a criterion for determining the share of participation of a homogeneous deformation in the total value of the cable deformation, the following ratio is proposed: $\chi = V(\pi)/V(0)$, where $V(\varphi)$ is the circumferential displacement of the outer surface of the body of the winding; $\varphi$ is the circumferential coordinate, the origin of which corresponds to the point where the cable descends.

The criterion for estimating the error of the formula in calculating the parameters of a homogeneous body denotes the following ratio: $\xi = V(0)/V_0$, here $V_0$ is the circumferential displacement of the outer surface of a homogeneous body corresponding to the stiffness (2).

To analyze the reaction of the body of the winding, taking into account a large share of the local displacements in the total value of the circumferential displacement, the dependence of the criteria $\chi$ and $\xi$ on $\sqrt{\rho_j}$ was investigated (Figs. 1, 2), using the following parameters of the RRC: $d = 4.2$ mm, $t = 20$ mm, $h = 10$ mm; as well as the winding parameter: $R_0 = 400$ mm. In the calculation, 4, 5, 6, 7, 8, 9, 10 and 15 turns were taken into account. It can be seen from the figures that if the share of homogeneous displacements is 0.375–0.55 of the maximum circumferential displacement of the body of
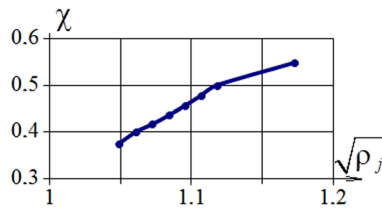
*Fig. 1. The curve for estimating the share of participation of the deformation homogeneity in the general index*
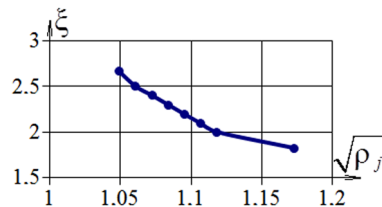


*Fig. 2. The curve for estimating the error of the formula for determining the stiffness of a homogeneous body*

the winding, then the error in calculating the stiffness according to (2) is 75−180 %. The criterion $Z$ varied from 33 to 65 at the same time.

During submarine mining, the belt of increased thickness can be used for improving the buoyancy of the drag heads. The computational experiment was based on the fact that the basic cable of the RRC-5000 has 5 turns of winding, and the radius of the shell $R_0 = 420$ mm. In comparison with the basic one (25.5 mm), the cable thickness varied in the range of 15−40 mm (Fig. 3). From the analysis of the graph it follows that the dependence of the $\chi$ criterion on $\sqrt{h}$ is close to the linear one.

To analyze the processes in the body of the winding, close to a homogeneous body, the bobbin winding RRC-5000 with a shell radius of $R_0 = 150$ mm is considered. At the same time, the number of turns varied in the range of 1...20 (Fig. 4).
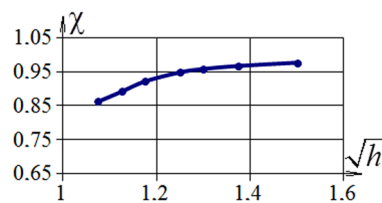


*Fig. 3. The curve for estimating the share of participation of the deformation homogeneity depending on the cable thickness in the overall index*
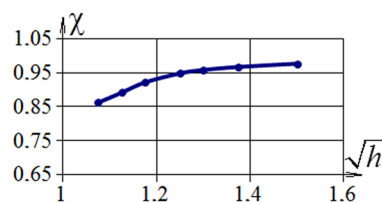


*Fig. 4. The curve for estimating the share of the participation of the deformation homogeneity in the general index as a function of the turns of the cable winding*

From the analysis of the figure it follows that for small values of the ratio $R_0/d$, even if the number of turns is small, the body of the winding during torsion shows itself as a homogeneous body.

In Fig. 5, two extreme cases of deformation of the body of the winding are demonstrated: close to homogeneous, when $\chi = 0/81$, and local deformation at which $\chi = 0/23$. According to (2), the stiffness of the body of the winding depends squarely on the outer diameter of its body, and the local value of this parameter depends little on the value of the diameter of the winding. Therefore, for a small number of turns, the stiffness of a homogeneous body exceeds the local stiffness, which causes a large error in the calculations using (2) (Fig. 2). However, in this case the value of the total winding compliance is of the same order as the compliance of the homogeneous body, that is, it is sufficiently small. The danger of dynamic effects occurring in the bobbin hoist during emergency and service braking occurs when there are a large number of turns in the winding, when the stiffness of a homogeneous body is much less than the local stiffness and the value of the total torsional stiffness of its body can be defined from (2) with the precision sufficient for dynamic analysis.

In the process of carrying out a series of computational experiments using the finite element model of the body of the winding, it turned out that the criterion ($Z = 20$) proposed by M. V. Polushina was not always consistent with the prevailing type of the deformed state. To make this criterion more precise an analytical model has been developed that takes into account the shear and compression of the soft rubber layers of the winding. In this model, the rope is presented in the form of an infinitely thin spiral and its stiffness characteristics correspond to the real element. The entire body of the winding is modeled as a cylinder, the reduced stiffness characteristics of which correspond to a reinforced spiral rope. Below we consider the algorithm for calculating these reduced characteristics.

**The definition of reduced stiffness characteristics of the body of the winding.** In Fig. 6 the result of solving the problem of defining the transverse compression of the RRC packet is shown, which is obtained in Panchenko›s papers. It can be seen from the figure that the expansion process of the body of the winding is affected by the expansion of the rubber near its free surface. Under the conditions of the torsion of the body of the winding, the
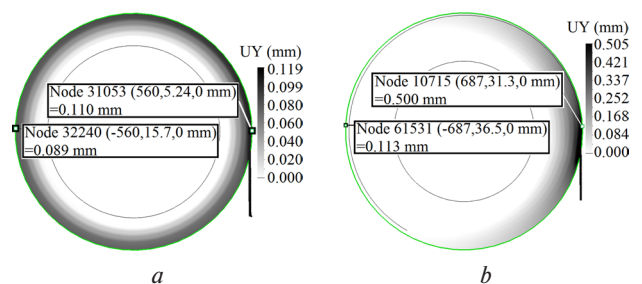


*Fig. 5. Indices of the characteristics of a deformed state of the body of the winding, if:*

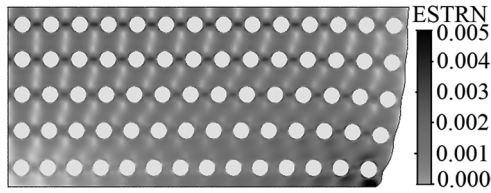$a − \chi = 0.81; b − \chi = 0.23$ (b)

*Fig. 6. Modeling of the process of transverse compression of the RRC packet*

stiffness of the system depends mainly on the work of the central part of the packet, which is 80 % of the total body volume of the winding. Therefore, to define the compressive stiffness of the packet, it is permissible to replace the rubber-rope cable with a set of non-interacting rubber-coated ropes, the stiffness characteristics of which correspond to the indices of the central part of the body of the winding, namely

$$B(\eta,\tau,i,j) = \begin{pmatrix} 0.660 + 0.520\cdot\eta + 0.210\cdot\tau - \\ -0.160\cdot\eta^2 + 0.240\cdot\eta\cdot\tau + 0.001\cdot\tau^2 \end{pmatrix} \times$$
$$\times \begin{pmatrix} 1 + 3.120\cdot1.900^{-(i-1)^{0.630}}\cdot(1-1.290^{i-j}) + \\ + 5.110\cdot1.570^{-(i-1)^{0.810}}\cdot1.290^{i-j} \end{pmatrix}, \quad (3)$$

where $\eta = 1/(h/d - 1)$, $\tau = 1/(t/d - 1)$; $i$ is the number of the winding turn in the packet; $j$ is the general number of the turns.

To solve the problem of defining the torsional stiffness of the RRC body of the winding, we use the method of computer finite element modeling.

For this purpose, we introduce the dimensionless integral characteristics of the $i$th winding layer in the RRC packet with the total number of layers $j$, among which the torsional stiffness coefficient of the body of the winding is

$$G' = P_y / (w_y \cdot G_r), \quad (4)$$

where $P_y$ is the distributed load acting on the $i$th layer, $w_y$ is the movement of the layer along the axis y (Fig. 7).

We define the value of the coefficient $G'$ depending on such parameters of the winding of the RRC: $t/d$, $h/d$, $i, j$.

We accept the following assumption: the coefficient of the torsional stiffness of the winding layer of the RRC has the form of a product of two coefficients, that is
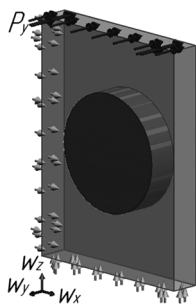
$$G' = G'' \cdot k_G, \quad (5)$$



*Fig. 7. The boundary conditions for a finite element model for defining the parameter G″*

where $G''$ is the coefficient of the torsional stiffness of the winding, taking into account only the geometry of the structure and the physical and mechanical properties of the components; $k_G$ is the coefficient of hardening of the winding layer of the RRC, which takes into account the edge effect when the cable touches the surface of the organ of the winding.

We find the value of $G''$. To do this, we carry out a computational experiment. In the finite element model (Fig. 7) the following boundary conditions are accepted: along the left edge of the modeled rectangle − the symmetry condition, along the lower one − the prohibition of vertical displacements, and along the upper edge in the longitudinal direction the force of 500 N/m is given.

**Defining the $G''$ parameter.** In the use of the finite element model, boundary conditions are set and the SST in the layer of the wound cable is defined. The results of the measurements are processed using (4). At the same time, the geometrical parameters of the RRC varied. The results of the computational experiments have been tabulated.

Considering the ratios $t/d$ and $h/d$ to be variables, we find an approximate function that connects them. The approximating polynomial for defining the torsional stiffness coefficient of the RRC body of the winding can be written as follows

$$G''(\eta, \tau) = s_1 + s_2\cdot\eta + s_3\cdot\tau + s_4\cdot\eta^2 + s_5\cdot\eta\cdot\tau + s_6\cdot\tau^2. \quad (6)$$

Here

$$\{s\}^T = \{s_1 \ s_2 \ s_3 \ s_4 \ s_5 \ s_6\}. \quad (7)$$

This is a vector of unknown quantities established by the method of least squares with minimizing the squares of the deviations of the polynomial $G''(\eta,\tau)$.

In this case

$$\Delta = \sum_{i=1}^{m}\sum_{j=1}^{n}(-G''_{i,j} + s_1 + s_2\cdot\eta_i + s_3\cdot\tau_j +$$
$$+ s_4\cdot\eta_i^2 + s_5\cdot\tau_j\cdot\eta_i + s_6\cdot\tau_j^2)^2,$$

where $m$, $n$ denote the number of rows and columns in the Table.

We find the partial derivatives of the value $\Delta$. Equating them to zero, we obtain the system of equations for defining the coefficients of the vector $\{s\}$, namely

*Table*

Values of the coefficient $G''$ depending on the geometrical parameters of the rubber-rope cable

| $h/d$ | $t/d$ | | | | | |
|---|---|---|---|---|---|---|
| | 1.200 | 1.300 | 1.400 | 1.600 | 1.800 | 2.000 |
| 1.700 | 4.172 | 3.151 | 2.642 | 2.144 | 1.895 | 1.740 |
| 1.900 | 3.725 | 2.827 | 2.369 | 1.926 | 1.702 | 1.567 |
| 2.100 | 3.388 | 2.591 | 2.182 | 1.781 | 1.525 | 1.456 |
| 2.300 | 3.117 | 2.405 | 2.038 | 1.675 | 1.490 | 1.377 |
| 2.500 | 2.893 | 2.254 | 1.920 | 1.596 | 1.421 | 1.316 |
| 2.700 | 2.702 | 2.126 | 1.821 | 1.520 | 1.363 | 1.266 |

$$\begin{cases}\dfrac{\partial}{\partial s_1}\Delta = \sum_{i=1}^{m}\sum_{j=1}^{n}\begin{pmatrix}-G''_{i,j}+s_1+s_2\cdot\eta_i+s_3\cdot\tau_j+\\+s_4\cdot\eta_i^2+s_5\cdot\tau_j\cdot\eta_i+s_6\cdot\tau_j^2\end{pmatrix}=0\\[6pt]\dfrac{\partial}{\partial s_2}\Delta = \sum_{i=1}^{m}\sum_{j=1}^{n}\begin{pmatrix}-G''_{i,j}+s_1+s_2\cdot\eta_i+s_3\cdot\tau_j+\\+s_4\cdot\eta_i^2+s_5\cdot\tau_j\cdot\eta_i+s_6\cdot\tau_j^2\end{pmatrix}\cdot\eta_i=0\\[6pt]\dfrac{\partial}{\partial s_3}\Delta = \sum_{i=1}^{m}\sum_{j=1}^{n}\begin{pmatrix}-G''_{i,j}+s_1+s_2\cdot\eta_i+s_3\cdot\tau_j+\\+s_4\cdot\eta_i^2+s_5\cdot\tau_j\cdot\eta_i+s_6\cdot\tau_j^2\end{pmatrix}\cdot\tau_j=0\\[6pt]\dfrac{\partial}{\partial s_4}\Delta = \sum_{i=1}^{m}\sum_{j=1}^{n}\begin{pmatrix}-G''_{i,j}+s_1+s_2\cdot\eta_i+s_3\cdot\tau_j+\\+s_4\cdot\eta_i^2+s_5\cdot\tau_j\cdot\eta_i+s_6\cdot\tau_j^2\end{pmatrix}\cdot\eta_i^2=0\\[6pt]\dfrac{\partial}{\partial s_5}\Delta = \sum_{i=1}^{m}\sum_{j=1}^{n}\begin{pmatrix}-G''_{i,j}+s_1+s_2\cdot\eta_i+s_3\cdot\tau_j+\\+s_4\cdot\eta_i^2+s_5\cdot\tau_j\cdot\eta_i+s_6\cdot\tau_j^2\end{pmatrix}\cdot\eta_i\cdot\tau_j=0\\[6pt]\dfrac{\partial}{\partial s_6}\Delta = \sum_{i=1}^{m}\sum_{j=1}^{n}\begin{pmatrix}-G''_{i,j}+s_1+s_2\cdot\eta_i+s_3\cdot\tau_j+\\+s_4\cdot\eta_i^2+s_5\cdot\tau_j\cdot\eta_i+s_6\cdot\tau_j^2\end{pmatrix}\cdot\tau_j^2=0\end{cases}.$$

We reduce this system to the standard form as follows

$$[A]\cdot\{s\}=\{C\}, \qquad (8)$$

where $\{s\}$ is a column vector of unknown quantities (7).

Next, we write down the matrix of the system (8) and the column vector of free terms

$$[A]=\begin{vmatrix}m\cdot n & \sum\limits_{i=1}^{m}\sum\limits_{j=1}^{n}\eta_i & \sum\limits_{i=1}^{m}\sum\limits_{j=1}^{n}\tau_j & \sum\limits_{i=1}^{m}\sum\limits_{j=1}^{n}\eta_j^2 & \sum\limits_{i=1}^{m}\sum\limits_{j=1}^{n}\eta_i\cdot\tau_j & \sum\limits_{i=1}^{m}\sum\limits_{j=1}^{n}\tau_j^2\\[10pt]\sum\limits_{i=1}^{m}\sum\limits_{j=1}^{n}\eta_i & \sum\limits_{i=1}^{m}\sum\limits_{j=1}^{n}\eta_j^2 & \sum\limits_{i=1}^{m}\sum\limits_{j=1}^{n}\eta_i\cdot\tau_j & \sum\limits_{i=1}^{m}\sum\limits_{j=1}^{n}\eta_j^3 & \sum\limits_{i=1}^{m}\sum\limits_{j=1}^{n}\eta_j^2\cdot\tau_j & \sum\limits_{i=1}^{m}\sum\limits_{j=1}^{n}\eta_i\cdot\tau_j^2\\[10pt]\sum\limits_{i=1}^{m}\sum\limits_{j=1}^{n}\tau_j & \sum\limits_{i=1}^{m}\sum\limits_{j=1}^{n}\eta_i\cdot\tau_j & \sum\limits_{i=1}^{m}\sum\limits_{j=1}^{n}\tau_j^2 & \sum\limits_{i=1}^{m}\sum\limits_{j=1}^{n}\eta_j^2\cdot\tau_j & \sum\limits_{i=1}^{m}\sum\limits_{j=1}^{n}\eta_i\cdot\tau_j^2 & \sum\limits_{i=1}^{m}\sum\limits_{j=1}^{n}\tau_j^3\\[10pt]\sum\limits_{i=1}^{m}\sum\limits_{j=1}^{n}\eta_j^2 & \sum\limits_{i=1}^{m}\sum\limits_{j=1}^{n}\eta_j^3 & \sum\limits_{i=1}^{m}\sum\limits_{j=1}^{n}\eta_j^2\cdot\tau_j & \sum\limits_{i=1}^{m}\sum\limits_{j=1}^{n}\eta_j^4 & \sum\limits_{i=1}^{m}\sum\limits_{j=1}^{n}\eta_j^3\cdot\tau_j & \sum\limits_{i=1}^{m}\sum\limits_{j=1}^{n}\eta_j^2\cdot\tau_j^2\\[10pt]\sum\limits_{i=1}^{m}\sum\limits_{j=1}^{n}\eta_i\cdot\tau_j & \sum\limits_{i=1}^{m}\sum\limits_{j=1}^{n}\eta_j^2\cdot\tau_j & \sum\limits_{i=1}^{m}\sum\limits_{j=1}^{n}\eta_i\cdot\tau_j^2 & \sum\limits_{i=1}^{m}\sum\limits_{j=1}^{n}\eta_j^3\cdot\tau_j & \sum\limits_{i=1}^{m}\sum\limits_{j=1}^{n}\eta_j^2\cdot\tau_j^2 & \sum\limits_{i=1}^{m}\sum\limits_{j=1}^{n}\eta_i\cdot\tau_j^3\\[10pt]\sum\limits_{i=1}^{m}\sum\limits_{j=1}^{n}\tau_j^2 & \sum\limits_{i=1}^{m}\sum\limits_{j=1}^{n}\eta_i\cdot\tau_j^2 & \sum\limits_{i=1}^{m}\sum\limits_{j=1}^{n}\tau_j^3 & \sum\limits_{i=1}^{m}\sum\limits_{j=1}^{n}\eta_j^2\cdot\tau_j^2 & \sum\limits_{i=1}^{m}\sum\limits_{j=1}^{n}\eta_i\cdot\tau_j^3 & \sum\limits_{i=1}^{m}\sum\limits_{j=1}^{n}\tau_j^4\end{vmatrix};\quad \{C\}=\begin{vmatrix}\sum\limits_{i=1}^{m}\sum\limits_{j=1}^{n}G'_{i,j}\\[8pt]\sum\limits_{i=1}^{m}\sum\limits_{j=1}^{n}G'_{i,j}\cdot\eta_i\\[8pt]\sum\limits_{i=1}^{m}\sum\limits_{j=1}^{n}G'_{i,j}\cdot\tau_j\\[8pt]\sum\limits_{i=1}^{m}\sum\limits_{j=1}^{n}G'_{i,j}\cdot\eta_i^2\\[8pt]\sum\limits_{i=1}^{m}\sum\limits_{j=1}^{n}G'_{i,j}\cdot\eta_i\cdot\tau_j\\[8pt]\sum\limits_{i=1}^{m}\sum\limits_{j=1}^{n}G'_{i,j}\cdot\tau_j^2\end{vmatrix}.$$

Using the Gaussian elimination method, we obtain the results of solving the system of equations (8) with three decimal places, that is

$$s^T=\{0.664\ \ 0.518\ \ 0.211\ -0.156\ \ 0.252\ \ 0.002\}. \quad (9)$$

Thus, the coefficients of the polynomial (6) are defined

$$G''(\eta,\tau)=0.664+0.518\cdot\eta+0.211\cdot\tau-$$
$$-0.156\cdot\eta^2+0.252\cdot\eta\cdot\tau+0.002\cdot\tau^2. \quad (10)$$

The coefficient $G''$ in expression (10) is defined taking into account the ratios $t/d$ and $h/d$, given in the table. Thus, this equation can be used to define torsional stiffness coefficient of the winding, taking into account only the geometry of the structure and the physical and mechanical properties of the components for series-produced standard sizes of RRC-1300−RRC-6000 belts.

**The definition of the coefficient $k_G$.** For this purpose, a stress-strain state in a packet from the RRC-3150 belt was studied by computational experiment, at the same time the number of layers of the belt in the packet was varied and the torsional stiffness coefficient of each layer was defined by (4). The edge effect that occurs when a layer of the ribbon contacts the surface of the organ of the winding was simulated in the boundary conditions by prohibiting vertical and horizontal movements of the lower edge of the RRC layer. Further we denote that $Gi,j$ is the torsional stiffness coefficient for of the $i^{\text{th}}$ layer in the packet with the total number of layers $j$. As a result of the calculations, the matrix $[G]$ was obtained.

Proceeding from (4), we define the hardening coefficient for the torsional stiffness parameter

$$k_{Gi,j}=G_{i,j}/G', \qquad (11)$$

and we obtain the matrix $[k_{Gi,j}]$. In order to generalize the results of calculations related to the elements of the matrix $[k_{Gi,j}]$, we find an approximating function of the following form

$$k_G(i,j)=1+k_1\cdot k_2^{-(i-1)^{k_3}}\cdot\left(1-k_4^{i-j}\right)+k_5\cdot k_6^{-(i-1)^{k_7}}\cdot k_4^{i-j}. \quad (12)$$

The values of the vector $\{k\}$ are defined by the method of least squares at the same time

$$k=\{3.279\ \ 1.964\ \ 0.651\ \ 1.318\ \ 5.617\ \ 1.556\ \ 0.791\}. \quad (13)$$

Taking into account the expressions (11−13), we obtain the final version of the equation for defining the torsional stiffness coefficient of the $i^{\text{th}}$ layer in the rubber-rope cable packet with the total number of layers $j$, that is

$$G'(\eta,\tau,i,j)=\begin{pmatrix}0.664+0.518\cdot\eta+0.211\cdot\tau-0.156\cdot\eta^2+\\+0.252\cdot\eta\cdot\tau+0.002\cdot\tau^2\end{pmatrix}\times$$
$$\times\begin{pmatrix}1+3.279\cdot1.964^{-(i-1)^{0.651}}\cdot\left(1-1.318^{i-j}\right)+\\+5.617\cdot1.556^{-(i-1)^{0.791}}\cdot1.318^{i-j}\end{pmatrix}. \quad (14)$$

The analytical expression used to define the torsional stiffness coefficient of the $i^{\text{th}}$ layer in the RRC package

with the total number of layers $j$ is suitable for calculating the parameters of the series-produced standard sizes of the RRC-1300 − RRC-6000 belts (Table).

**Analytical model of the RRC body of the winding.** We model the winding in the form of a hollow cylinder of homogeneous orthotropic material reinforced with an infinitely thin spiral, the pitch of which is equal to the thickness of the cable and the stiffness characteristics correspond to the indices of the rope. We will assume that in the radial direction the body of the winding experiences an unconstrained compression, characterized by a variable along the radius modulus of elasticity, which is defined from the following expression: $E_i = E_r \cdot B(\eta, \tau, i, j)$, where $E_r$ is the modulus of elasticity of the rubber.

Similarly for the shear modulus $G_i = G_r \cdot G'(\eta, \tau, i, j)$, where $G_r$ is the shear modulus of the rubber.

Since the stiffness of the rope is many times higher than the stiffness of the corresponding rubber layer, then, defining the potential deformation energy in torsion of the body of the winding, we can limit ourselves to three components of the total potential energy, that is $\Pi = \Pi_c + \Pi_r + \Pi_\gamma$, where $\Pi_c$ is the total potential energy of the rope extension; $\Pi_r$ and $\Pi_\gamma$ are the total potential energy of compression and shear of winding turns.

In the polar coordinate system it is convenient to characterize the displacement of the rope by the value of the angle of rotation of its turn, which corresponds to the following ratio: $\theta = V/r$, where $V$ is the circumferential displacement of the rope; $r$ is the radius of the spiral.

Extension strain of the rope is

$$\varepsilon_\varphi = \theta' + (u/r), \qquad (15)$$

where $\theta'$ is the derivative of the value $\theta$ with respect to the circumferential coordinate $\varphi$; $u$ is the radial displacement of the rope.

We denote extension force of the rope by $N$, defining this parameter as follows

$$N = B_c \cdot \varepsilon_\varphi, \qquad (16)$$

where $B_c$ is the extension stiffness of the rope.

The rope has the form of an Archimedean spiral, which means

$$r(\varphi) = r(0) + (h \cdot \varphi/2\pi).$$

As well as the ratio $(h/R_0) \ll 1$, the derivative $r(\varphi)'$ can be neglected. We will assume that $r_i(\varphi) = r_i(0) = R_0 + h \cdot (i + 0.5)$ if $i = 1, ..., j + 1$.

Variation of the total potential energy of rope extension is

$$\delta\Pi_c = \sum_{i=1}^{j} \int_0^{2\pi} N_i \cdot r_i \cdot \delta\varepsilon_{\varphi i} d\varphi = \sum_{i=1}^{j} \int_0^{2\pi} (N_i \cdot r_i) \cdot \left(\delta\theta_i + \frac{\delta u_i}{r_i}\right) d\varphi =$$

$$= \sum_{i=1}^{j} \left( \begin{array}{l} N_i(2\pi) \cdot r_{i+1} \cdot \delta\theta_i(2\pi) - N_i(0) \cdot r_i \cdot \delta\theta_i(0) - \\ -\int_0^{2\pi} N_i' \cdot r_i \cdot \delta\theta_i d\varphi + \int_0^{2\pi} N_i \cdot \delta u_i d\phi \end{array} \right).$$

We will also assume that the deformations of the matrix of anisotropic material are constant in the space between the turns of the ropes, they have the following values

$$\varepsilon_{r1} = \frac{2u_1}{h}; \quad \varepsilon_{ri} = \frac{u_i - u_{i-1}}{h}, \quad \text{if} \quad i = 2, ..., j;$$

$$\gamma_1 = \frac{u_1'}{R_1} + R_1 \cdot \frac{2 \cdot \theta_1}{h}; \quad \gamma_i = \frac{u_i' + u_{i-1}'}{2 \cdot R_i} + R_i \cdot \frac{\theta_i - \theta_{i-1}}{h}, \qquad (17)$$

$$\text{if} \quad i = 2, ..., j,$$

here $R_i = R_0 = (i - 1) \cdot h$.

These strain values correspond to the stresses defined from such expressions

$$\sigma_{ri} = E_i \cdot \varepsilon_{ri}; \quad \tau_i = G_i \cdot \gamma_i. \qquad (18)$$

Variation of the potential tensile energy of the matrix is

$$\delta\Pi_r = t \cdot h \cdot \int_0^{2\pi} \left( 0.5 \cdot R_1 \cdot \sigma_{r1} \cdot \delta\varepsilon_{r1} + \sum_{i=2}^{i} R_i \cdot \sigma_{ri} \cdot \delta\varepsilon_{ri} \right) d\varphi =$$

$$= t \cdot \int_0^{2\pi} \left( R_1 \cdot \sigma_{r1} \cdot \delta u_1 + \sum_{i=2}^{i} R_i \cdot \sigma_{ri} \cdot (\delta u_i - \delta u_{i-1}) \right) d\varphi.$$

Variation of the potential shear energy of the matrix is

$$\delta\Pi_\gamma = t \cdot h \cdot \int_0^{2\pi} \left( 0.5 \cdot R_1 \cdot \tau_1 \cdot \delta\gamma_1 + \sum_{i=2}^{i} R_i \cdot \tau_i \cdot \delta\gamma_i \right) d\varphi =$$

$$= t \cdot \left[ \begin{array}{l} R_1 \cdot \tau_1 \cdot \delta\left( \frac{u_1' \cdot h}{2 \cdot R_1} + R_1 \cdot \theta_1 \right) + \\ +\sum_{i=2}^{i} R_i \cdot \tau_i \cdot \delta\left( \frac{h \cdot (u_i' + u_{i-1}')}{2 \cdot R_i} + R_i \cdot (\theta_i - \theta_{i-1}) \right) \end{array} \right]_0^{2\pi} +$$

$$+ t \cdot \int_0^{2\pi} \left[ \begin{array}{l} -\tau_1' \cdot \delta\frac{u_1 \cdot h}{2} + R_1^2 \cdot \tau_1 \cdot \delta\theta_1 + \\ +\sum_{i=2}^{i} \left\{ -\tau_i' \cdot \delta\frac{h \cdot (u_i + u_{i-1})}{2} + \tau_i \cdot R_i^2 \cdot \delta(\theta_i - \theta_{i-1}) \right\} \end{array} \right] d\varphi.$$

On the basis of certain equations we obtain the equilibrium equations, that is

$$N_i' \cdot r_i - t \cdot R_i^2 \cdot \tau_i + t \cdot R_{i+1}^2 \cdot \tau_{i+1} = 0, \quad \text{if} \quad i = 1, ..., j-1;$$

$$N_j' \cdot r_j - t \cdot R_j^2 \cdot \tau_j = 0; \qquad (19)$$

$$N_i + t \cdot R_i \cdot \sigma_{ri} - t \cdot R_{i+1} \cdot \sigma_{ri+1} - 0.5 \cdot t \cdot h \cdot (\tau_i' + \tau_{i+1}') = 0;$$

$$N_i + t \cdot R_i \cdot \sigma_{ri} - 0.5 \cdot t \cdot h \cdot \tau_i' = 0. \qquad (20)$$

We write the boundary conditions for the obtained parameters

$$\theta_1(0) = 0; \quad u_1(0) = 0; \quad N_j(2\pi) = P;$$

$$\theta_i(0) = \theta_{i-1}(2\pi), \quad \text{if} \quad i = 2, ..., j;$$

$$N_i(0) = N_{i-1}(2\pi), \quad \text{if} \quad i = 2, ..., j;$$

$$u_i(0) = u_{i-1}(2\pi), \quad \text{if} \quad i = 2, ..., j; \qquad (21)$$

$$\tau_i(0) = \tau_{i-1}(2\pi), \quad \text{if} \quad i = 2, ..., j,$$

where $P$ is the additional tension force of the cable.

Substituting expressions (15−18) into equations (19), (20), we obtain the systems of linear equations with constant coefficients, namely

$$\begin{cases} B_c \cdot \left(\theta_1'' \cdot r_1 + u_1'\right) - t \cdot R_1^2 \cdot G_1 \cdot \left(\dfrac{u_1'}{R_1} + R_1 \cdot \dfrac{2 \cdot \theta_1}{h}\right) + \\[2mm] + t \cdot R_2^2 \cdot G_2 \cdot \left(\dfrac{u_2' + u_1'}{2 \cdot R_2} + R_2 \cdot \dfrac{\theta_2 - \theta_1}{h}\right) = 0 \\[3mm] B_c \cdot \left(\theta_i'' \cdot r_i + u_i'\right) - t \cdot R_i^2 \cdot G_i \cdot \left(\dfrac{u_i' + u_{i-1}'}{2 \cdot R_i} + R_i \cdot \dfrac{\theta_i - \theta_{i-1}}{h}\right) + \\[2mm] + t \cdot R_{i+1}^2 \cdot G_{i+1} \cdot \left(\dfrac{u_{i+1}' + u_i'}{2 \cdot R_{i+1}} + R_{i+1} \cdot \dfrac{\theta_{i+1} - \theta_i}{h}\right) = 0 \\[3mm] B_c \cdot \left(\theta_j'' \cdot r_j + u_j'\right) - t \cdot R_j^2 \cdot G_j \cdot \left(\dfrac{u_j' + u_{j-1}'}{2 \cdot R_j} + R_j \cdot \dfrac{\theta_j - \theta_{j-1}}{h}\right) = 0 \end{cases} ; \quad (22)$$

$$\begin{cases} B_c \cdot \left(\theta_1' + \dfrac{u_1}{r_1}\right) + t \cdot R_1 \cdot E_1 \cdot \dfrac{2u_1}{h} - t \cdot R_2 \cdot E_2 \cdot \dfrac{u_2 - u_1}{h} - \\[2mm] - 0.5 \cdot t \cdot h \cdot \left\{ \begin{aligned} & G_1 \cdot \left(\dfrac{u_1'}{R_1} + R_1 \cdot \dfrac{2\theta_1}{h}\right) + \\ & + G_2 \cdot \left(\dfrac{u_2' + u_1'}{2R_2} + R_2 \cdot \dfrac{\theta_2 - \theta_1}{h}\right) \end{aligned} \right\} = 0 \\[4mm] B_c \cdot \left(\theta_i' + \dfrac{u_i}{r_i}\right) + t \cdot R_i \cdot E_i \cdot \dfrac{u_i - u_{i-1}}{h} - t \cdot R_{i+1} \cdot E_{i+1} \cdot \dfrac{u_{i+1} - u_i}{h} - \\[2mm] - 0.5 \cdot t \cdot h \cdot \left\{ \begin{aligned} & G_i \cdot \left(\dfrac{u_i' + u_{i-1}'}{2R_i} + R_i \cdot \dfrac{\theta_i - \theta_{i-1}}{h}\right) + \\ & + G_{i+1} \cdot \left(\dfrac{u_{i+1}' + u_i'}{2R_{i+1}} + R_{i+1} \cdot \dfrac{\theta_{i+1} - \theta_i}{h}\right) \end{aligned} \right\} = 0 \\[4mm] B_c \cdot \left(\theta_j' + \dfrac{u_j}{r_j}\right) + t \cdot R_j \cdot E_j \cdot \dfrac{u_j - u_{j-1}}{h} - \\[2mm] - 0.5 \cdot t \cdot h \cdot G_j \cdot \left(\dfrac{u_i' + u_{i-1}'}{2R_j} + R_j \cdot \dfrac{\theta_j - \theta_{j-1}}{h}\right) = 0 \end{cases} \quad (23)$$

with $i = 2, \ldots, j - 1$.

The general result of solving the systems of equations (19) and (20) has the following form

$$\begin{aligned} \theta_i(\varphi) &= \sum_{k=1}^{j} C_{\theta j} \cdot a_{kj} \cdot e^{\lambda_k \cdot \varphi} + \sum_{k=1}^{j} D_{\theta j} \cdot a_{kj} \cdot e^{-\lambda_k \cdot \varphi}; \\ u_i(\varphi) &= \sum_{k=1}^{j} C_{uj} \cdot b_{kj} \cdot e^{\lambda_k \cdot \varphi} + \sum_{k=1}^{j} D_{uj} \cdot b_{kj} \cdot e^{-\lambda_k \cdot \varphi}, \end{aligned} \quad (24)$$

where $\lambda_k$, $a_{kj}$, $b_{kj}$ are the roots and elements of the matrix of the functions of the forms of the characteristic systems of equations (22, 23); $C_{\theta j}$, $D_{\theta j}$, $C_{uj}$, $D_{uj}$, are the integration constants that are defined from the boundary conditions.

We analyze the structure of the systems of equations (22) and (23). The system (22) contains the parameter which is proportional to the following ratio

$$\kappa^2 = \dfrac{B_c \cdot R_j \cdot h}{t \cdot R_0^3 \cdot G_j}. \quad (25)$$

It occurs at the second derivatives. Therefore, the rate of decay of the solution in the vicinity of the point of the cable descend is proportional to the value $e^{\kappa \varphi}$. In system (23), the similar parameter determines the relationship between the values $\theta$ and $u$. The parameters at the second derivatives are of the order of unity. Hence it

follows that it is permissible to solve systems (22, 23) by an iteration method. At the first stage we assume that the radial displacements of the rope are equal to zero in system (22). At the second stage the corresponding radial values are found from system (23) from the found values of the circumferential displacements. The error in the results of applying the iteration method relative to the real ranges of the RRC and the bobbin winding did not exceed 10 %. The results of computational experiments covering the change in the ratios of the parameters $h/d$, $t/d$, $R_0/d$, $r_j/R_0$, $B_c/G \cdot t \cdot R_0$, are shown in Fig. 8.

We define the stiffness characteristics for the shear of the experimental sample of the rubber-rope cable RRC-1300 on a tearing machine (Fig. 9). According to the testing program, the samples 500 mm long were made from RRC-1300. One rope of the cable was clamped in the upper plunger, and the second − in the lower one, then stretched in the range from 2035 to 14250 MPa. During the loading process the deformations of the sample were measured.

For each experiment the value of the magnitude of the shear modulus of the rubber cable matrix $G$ was calcula-
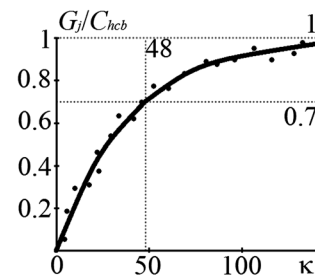


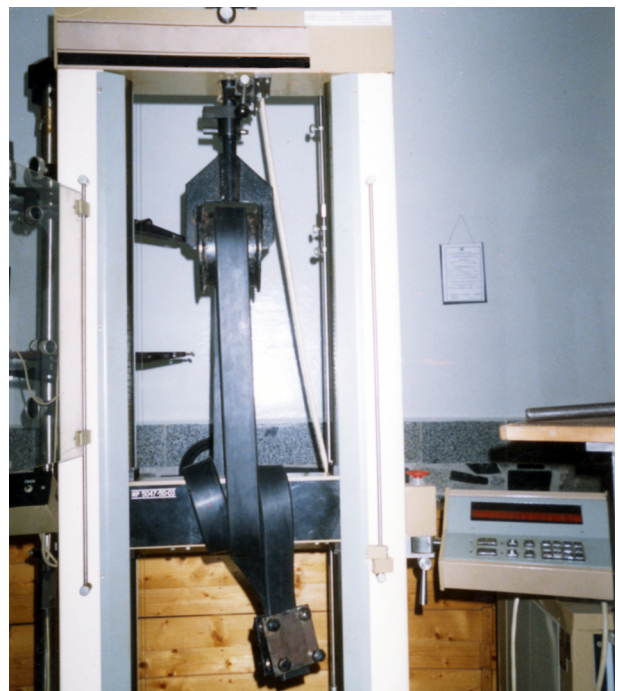Fig. 8. The dependence curve of Gj/Chcb on the parameter κ



Fig. 9. The testing of the rope on the tearing machine

ted. After a set of values had been obtained, they were checked for crude errors. The root-mean-square deviation $\sigma^*$ for the $G$ value was 1 MPa. As well as in the previous experiments, the homogeneity of the variance of the results and the influence of the factor on the response were proved. It was also concluded that the distribution of the cable shear modulus in the sampling obeys the normal law and at a confidence probability of 95 % the deviation of the limits of the confidence interval from the mathematical expectation is 0.9 %, that is $G = (1 \pm 0.009)$ MPa.

Fig. 10 shows a schematic diagram of an experimental plant for defining the shear stiffness of the body of the winding of the rubber-rope cable. The following parameters of the body of the winding were used: the coefficient of longitudinal stiffness of the winding layer $B_c = 6658$; the cable shear modulus $G = 1$ MPa; cable thickness $h = 10$ mm; cable width $b = 43$ mm; the number of ropes in the cables is 2; initial radius of the bobbin $R_0 = 500$ mm; the number of turns in the winding is 20.

The shear stiffness was determined by measuring the deformation of the body of the winding after loading and unloading. On bobbin 9, under the influence of load 1 weighing $Q$ cable 2 was wound up to the necessary radius $R$, then it was loaded up to 500 N. For this purpose, additional loads 3 were hung to wire rope clips 4 in the following order: 100 N, 100 N, 200 N, 100 N. At the same time, using a dial gauge 5, linear displacement of the cable was measured, which ran on the bobbin. This indicator is connected with the cable by a thin wire, which is attached to wire rope clips 6. The latter ones slided along the cable guides. Then the loads were taken off in the reverse order and the unloading of the body of the winding was made. The thread, on which the loads weighing from 100 to 300 N were hung up, was thrown over pulley 7. The cycle of loading-unloading was repeated 5–6 times. The experiment was carried out while changing the tension of the cable $Q$, under the action of which the winding takes place. Since the experimental plant includes the series connection of two links, each of which has different stiffness (the bobbin organ of the winding of the RRC and the string of the cable), the value of the given parameter with regard to the RRC body of the winding is calculated according to the following formula

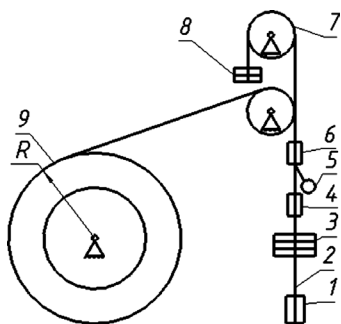$$C_{hcb} = \frac{C_{st} \cdot C_{equiv}}{C_{st} - C_{equiv}},$$

where $C_{equiv}$ is the equivalent value of the stiffness of the computational scheme preconditioned by the indices of the indicator; $C_{st}$ is the stiffness of the string of the cable ($C_{st} = B_c/L = 14.5$ MN/mm if $L = 10$ m).

As well as in the previous cases, the tests showed homogeneity of the variance of the results and the influence of the factor on the response. An analytical dependence of the stiffness of the RRC body of the winding has also been established and the law of distribution of its parameters by the Pearson criterion has been revealed.

Fig. 11 shows the graphical schemes of the dependence of the displacement on the loading of the upper layer of the cable under the conditions of cyclic loading and unloading of the body of the winding of the first type. In this case the curves of cyclic deformation are characterized by a relatively small area of the hysteresis loop; almost full repetition of the shape of the loop during the consequent cycles of the loading; approximately the same dependence of the displacement on the loading and unloading forces. These facts indicate that there is no slipping of the turns of the winding, as well as the belonging of the object under investigation to linear elastic solid bodies.

In Fig. 12 the graphs of dependencies of the body of the winding stiffness on the parameter $\rho$ ($\rho = R_0/R_{max}$) for different values of the $\kappa$ criterion are built. Here the curve of the reduced theoretical dependence $C_\text{T} = f(\rho)$ is also shown. It is built taking into account the results of the calculating formula for the parameters of the cable RRC-1300. The graphs illustrate two different mechanisms of deformation of the body of the winding, depending on the value of the $\kappa$ criterion, which coincides with the conclusions obtained theoretically. For example, if $\kappa \geq 48$, then the curves of the experimental and theoretical dependence of the stiffness on the $\rho$ param-
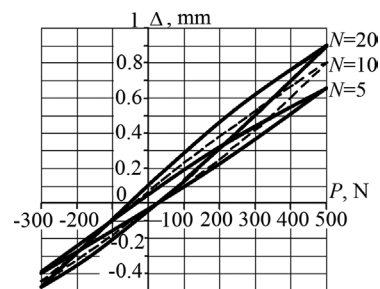


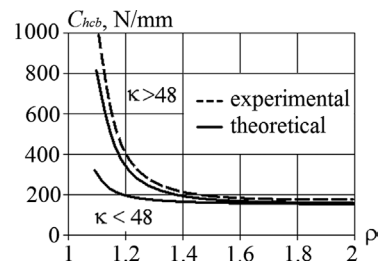*Fig. 11. The curves of the dependence of the cable displacements on the loading*



*Fig. 12. The curves of the dependence of the stiffness of the rubber-rope cable winding on its reduced radius*



*Fig. 10. The scheme of the experimental plant for studying the winding of the rubber-rope cable*

eter almost coincide. The maximum deviation takes place for a small number of turns and is 16 %.

Summarizing the results of studies of the model of the bobbin organ of the winding, it is possible to draw the following conclusions:

1. The nonlinear character of changing the reduced stiffness characteristics of the RRC packet layers is caused by the peculiarity of the interaction of the first layer of the packet with the surface of the bobbin. This interaction can be taken into account by applying the coefficient of a torsional stiffness hardening, for which an analytical expression is obtained by processing the results of a computational experiment. The equations are suitable for calculating the parameters of the series-produced standard sizes of the RRC-2500 − RRC-6000 belts.

2. An analytical model has been developed that takes into account the shear and compression of the soft rubber layers of the cable. In this model the rope is presented in the form of an infinitely thin spiral, the stiffness characteristics of which correspond to the real element. The entire body of the winding is modeled as a cylinder, the reduced stiffness characteristics of which correspond to a reinforced spiral rope.

3. The stiffness of the body of the winding depends quadratically on its outer diameter, and the local stiffness depends little on the diameter value. Therefore, for a small number of turns, the stiffness of a homogeneous body exceeds local stiffness. However, in this case the value of the total compliance is of the same order as the compliance of the homogeneous body, i.e. it is small enough. The danger of dynamic effects occurring in the bobbin hoist during emergency and service braking occurs with a large number of turns in the winding when the stiffness of the homogeneous body is much less than the local stiffness and the value of the total torsional stiffness of the body of the winding can be defined by the proposed formula with the precision sufficient for dynamic analysis.

4. To distinguish between the local and homogeneous mechanism of the reaction of the body of the winding the criterion κ is proposed, the value of which is directly proportional to the square roots of the longitudinal stiffness of the rope, the outer radius of the winding, as well as the cable thickness, and inversely proportional to the square roots of the packaging pitch of the ropes in the cable, to the cube roots of the radius of the shell and the value of the reduced torsional stiffness of the matrix of the body of the winding. The most characteristic value, which separates both types of the reaction of the winding, was considered to be κ = 48.

### References.
**1.** Franchuk, V. P., Ziborov, K. A., Krivda, V. V. and Fedoriachenko, S. O., 2017. On wheel rolling along the rail regime with longitudinal load. *Naukovyi Visnyk Natsionalnoho Hirnychoho Universytetu*, 3, pp. 62−67.
**2.** Bondarenko, V. I., Samusya, V. I. and Smolanov, S. N., 2005. Mobile lifting units for wrecking works in pit shafts. *Gornyi Zhurnal* [online], 5, pp. 99−100. Available at: <https://www.researchgate.net/publica-tion/293115005_Mobile_lifting_units_for_wrecking_works_in_pit_shafts> [Accessed 11 July 2017].
**3.** Ilin, S. R., Samusia, V. I., Ilina, I. S. and Ilina, S. S., 2016. Influence of dynamic processes in mine hoists on safety exploitation of shafts with broken geometry. *Naukovyi Visnyk Natsionalnoho Hirnychoho Universytetu*, 3, pp. 42−47.
**4.** Taran, I. and Klymenko, I., 2017. Analysis of hydrostatic mechanical transmission efficiency in the process of wheeled vehicle braking. *Transport Problems, 12/Special Edition*, pp. 45−56.
**5.** Kolosov, D., Dolgov, O. and Kolosov, A., 2013. The stress-strain state of the belt on a drum under compression by flat plates. In: *Annual Scientific-Technical Collection. Mining of Mineral Deposits*, pp. 351−357.
**6.** Zabolotnyi, K., Zhupiiev, O. and Molodchenko, A., 2018. The effect of stiffness of shoe brake elements on the distribution of contact pressures. *Naukovyi Visnyk Natsionalnoho Hirnychoho Universytetu*, 2, pp. 39−45. DOI: 10.29202/nvngu/2018-2/8.

## Вплив параметрів гумотросового канату на крутильну жорсткість тіла намотки

*К. С. Заболотний, О. В. Панченко, О. Л. Жупієв, М. В. Полушина*

Державний вищий навчальний заклад „Національний гірничий університет“, м. Дніпро, Україна, e-mail: mmf@ua.fm

**Мета.** Розробка математичної моделі напружено-деформованого стану тіла намотки бобінних підіймальних машин із гумотросовим канатом.

**Методика.** Використані методи математичного та обчислювального експерименту на основі скінченно-елементного аналізу.

**Результати.** Розв'язуючи задачі на визначення крутильної жорсткості тіла намотки гумотросового канату (ГТК), фізичну модель її бобінного органа уявили у вигляді композиту, де армування канату вважається нескінченно тонкою спіраллю із жорсткісними характеристиками металевого троса, а матриця — гумовою оболонкою. Після обробки результатів обчислювального експерименту з визначення параметрів тіла намотки ГТК, здійсненого методом комп'ютерного скінченно-елементного моделювання, отримали аналітичний вираз для розрахунку її коефіцієнта жорсткості на кручення, з якого випливає висновок про квадратичну залежність між жорсткістю тіла намотки та її зовнішнім діаметром, причому локальна жорсткість конструкції від значення діаметра залежить несуттєво. Небезпека виникнення в бобінах підіймника динамічних ефектів може мати місце, коли намотка має багато витків.

**Наукова новизна.** Встановлені закономірності впливу параметрів гумотросового канату на крутильну жорсткість тіла його намотки. Нелінійний характер зміни розглянутих характеристик жорсткості кожного шару намотки в пакеті ГТК викликаний особливістю взаємодії першого шару з поверхнею бобіни. Цю взаємодію можна простежити,

застосовуючи коефіцієнт посилення жорсткості на кручення, обчислюваний за допомогою отриманого шляхом обробки результатів обчислювального експерименту аналітичного виразу.

**Практична значимість.** Розроблена математична модель визначення жорсткості намотки гумотросового канату дозволяє знаходити такі значення параметрів бобінного підйомника, що дозволять уникнути небезпеки появи динамічних ефектів під час аварійного та робочого гальмування пристрою, викликаних крутильною жорсткістю тіла намотки.

**Ключові слова:** *бобінна підіймальна машина, гумотросовий канат, багатошарова намотка, тіло намотки, крутильна жорсткість намотки*

## Влияние параметров резинотросового каната на крутильную жесткость тела намотки

*К. С. Заболотный, Е. В. Панченко, А. Л. Жупиев, М. В. Полушина*

Государственное высшее учебное заведение „Национальный горный университет“, г. Днепр, Украина e-mail: mmf@ua.fm

**Цель.** Разработка математической модели напряженно-деформированного состояния тела намотки бобинных подъемных машин с резинотросовым канатом.

**Методика.** Использованы методы математического и вычислительного эксперимента на основе конечно-элементного анализа.

**Результаты.** Для решения задачи по определению жесткости на кручение тела намотки резинотросового каната (РТК) физическую модель ее бобинного органа представили в виде композита, считая армировку каната бесконечно тонкой спиралью, имеющей жесткостные характеристики ме-
таллического троса, а матрицу — резиновой оболочкой. После обработки результатов вычислительного эксперимента по определению параметров тела намотки РТК с использованием метода компьютерного конечно-элементного моделирования было получено аналитическое выражение для расчета ее коэффициента жесткости на кручение, из которого следует вывод о квадратичной зависимости между жесткостью тела и ее наружным диаметром, причем локальная жесткость конструкции от значения диаметра зависит несущественно. Опасность возникновения в бобинном подъемнике динамических эффектов может иметь место при большом числе витков в намотке.

**Научная новизна.** Установлены закономерности влияния параметров резинотросового каната на крутильную жесткость тела его намотки. Нелинейный характер изменения жесткостных характеристик каждого слоя намотки в пакете РТК вызван особенностью взаимодействия первого слоя с поверхностью бобины. Это взаимодействие можно проследить, применяя коэффициент увеличения жесткости на кручение, вычисляемый из полученного путем обработки результатов вычислительного эксперимента аналитического выражения.

**Практическая значимость.** Разработанная математическая модель определения жесткости намотки резинотросового каната позволяет находить такие значения параметров бобинного подъемника, при которых будет исключена опасность появления динамических эффектов во время аварийного и рабочего торможения устройства, вызванных крутильной жесткостью тела намотки.

**Ключевые слова:** *бобинная подъемная машина, резинотросовый канат, многослойная намотка, тело намотки, крутильная жесткость намотки*